Electronic Supplementary Material (ESI) for Nanoscale.

Enhanced Surface Stabilization of Gold Nanoclusters through Diglyme Coordination

Ian D. Anderson, Yuchen Wang, Christine M. Aikens, Christopher J. Ackerson

Experimental Methods

Synthesis of $Au_{25}(PET)_{18}$. A previously published method was adapted for the synthesis of $Au_{25}(PET)_{18}TOA$.[1] In brief, 2.0 g $HAuCl_4•3H_2O$ and 3.12 g tetra-*n*-octylammonium bromide were added to 140 mL tetrahydrofuran in a 300 mL roundbottom flask. The solution was stirred for 30 minutes until a dark orange color was observed. 3.6 mL of 2-phenylethanethiol was then added to the flask, and the resulting solution was stirred overnight. A separate solution containing 1.94 g sodium borohydride and 48 mL H_2O was produced in a 125 mL Erlenmeyer flask. This solution was cooled to 0 ˚C prior to adding it to the gold-containing solution. The combined solutions were then stirred for 48 hours, followed by separation and evaporation of the organic layer. The resulting brown oil was re-dissolved in several milliliters of dichloromethane and separated into four 50 mL conical vials. The conical vials were filled with methanol and placed in a centrifuge at 4000 RPM for 30 minutes. The supernatant was decanted and the precipitate was washed twice more by addition of methanol and centrifugation. The final product was extracted from the resulting powder using dichloromethane and dried in order to oxidize the cluster from its native -1 charge state to neutral.

Synthesis of $[Au_{20}(PET)_{15}(DG)_2]·4[DG]$. Synthetic conditions were adapted from a previously published report.[2] In brief, 48 mL of THF was added to a 250 mL Erlenmeyer flask followed by 643 µL of 2-phenylethanethiol (4.8 mmol, 3 eq). 630 mg $HAuCl_4•3H_2O$ (1.6 mmol, 1 eq) dissolved in 16 mL diglyme was added to the reaction vessel under constant magnetic stirring. Over the course of 3 hours the initial cloudy yellow solution transitioned to a completely opaque milky white. Approximately five minutes prior to the end of this 3 hour period, a suspension of 15.1 mg sodium borohydride (0.4 mmol, 0.25 eq) in 4 mL diglyme was sonicated at room temperature. At the 3 hour mark this suspension was then added dropwise over the course of 1 minute, followed by 120 mL diglyme. During the sodium borohydride addition, the solution turned dark black but quickly transitioned to a deep orange following the addition of the gross excess of diglyme. The reaction was stirred for an additional hour, whereupon the solution was passed through a Büchner funnel with a medium frit to remove insoluble byproducts. Quenching was performed by transferring this filtered solution to a 1-L fleaker and adding methanol to 1 L. The precipitated nanocluster product was isolated as an orange solid by passing this quenched solution through a Büchner funnel with a fine frit and further rinsing with excess methanol. For solution-phase studies, this solid product was dried overnight and re-suspended in either dichloromethane or chloroform. Yield was calculated with reference to the precursor gold salt $HAuCl_4•3H_2O$ and the full cluster formula, including the 4 excess diglyme.

Hierarchical Assembly Test. In a typical experiment, a 20 mg/mL solution of nanocluster sample in 2 mL chloroform was stored in a 5-mL scintillation vial and covered with a thin layer of parafilm to allow for the safe dispersal of any vapor. This vial was submerged halfway in a Büchi B-100 water bath set to the desired temperature (30 °C, 40 °C, 50 °C, or 60 °C) and held in place by a clamp for the duration of one hour. The vial was then removed and placed within an ice water bath in order to rapidly cool the solution prior to analysis by UV/Vis linear absorption spectroscopy. For each temperature, additional experiments were performed with an excess (2 mL) of diglyme added to the 2 mL nanocluster solutions, providing a total of eight experiments.

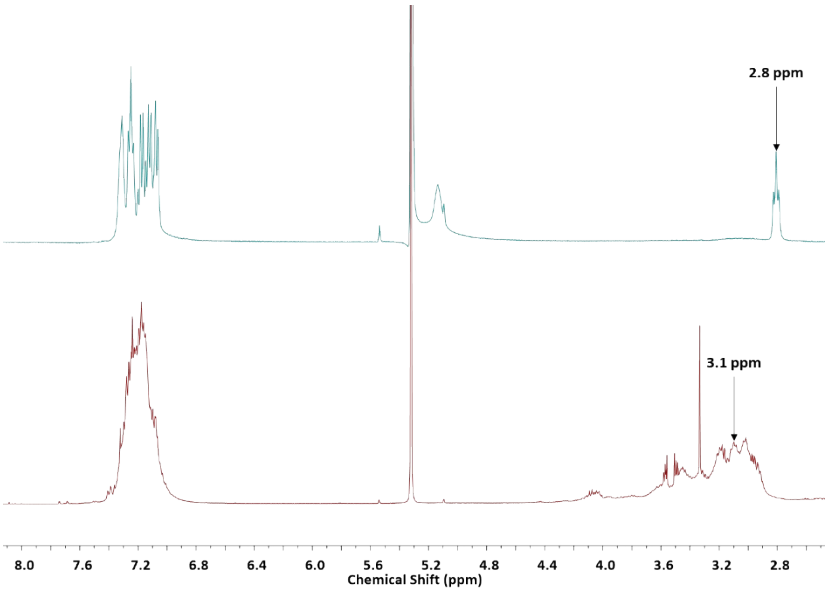

Figure S1: ^1H spectra of $Au_{25}(PET)_{18}$ (top, blue) and $[Au_{20}(PET)_{15}(DG)_2]·4[DG]$ (bottom, red) in dichloromethane-d_2. The central position of the peaks corresponding to the ethylene linker protons of PET are indicated for both samples.

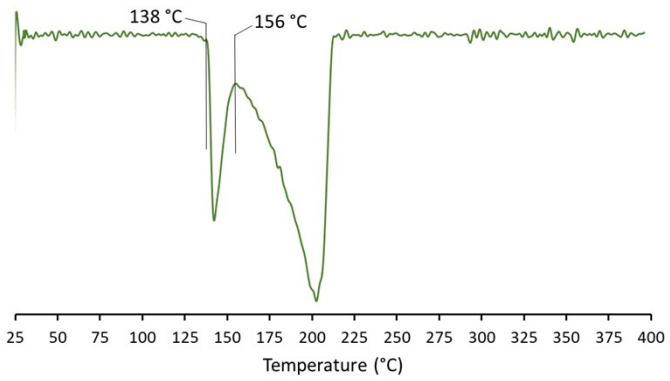

Figure S2: Differential thermal analysis (DTA) plot of the TGA data for $[Au_{20}(PET)_{15}(DG)_2]\cdot 4[DG]$, obtained by taking the difference of every adjacent pair of weight % values and dividing by the time change. The raw DTA values were smoothed using a Savitzky-Golay filter with a window of 10 °C.

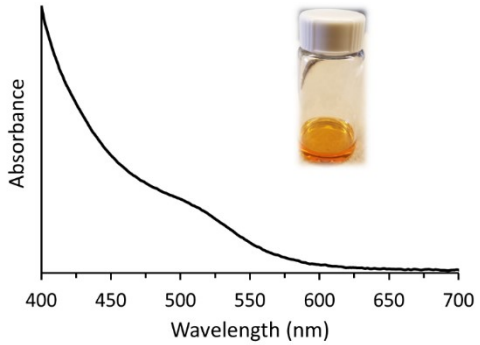

Figure S3: Linear absorption spectrum of $[Au_{20}(PET)_{15}(DG)_2]\cdot 4[DG]$ in chloroform. Inset shows a 10 mg/mL solution of the nanocluster, showcasing its gold-orange hue.

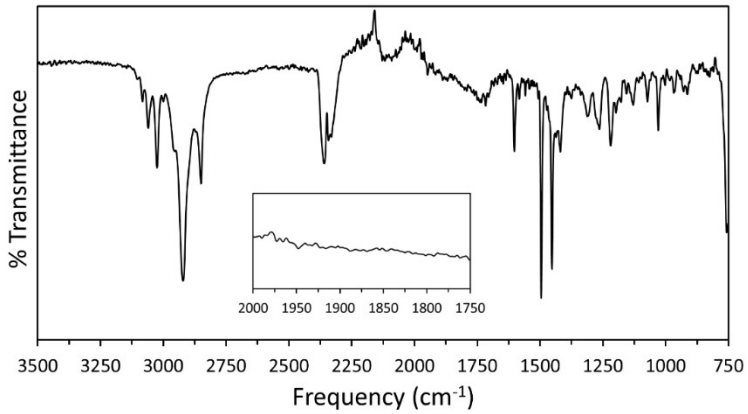

Figure S4: FT-IR spectrum of $[Au_{20}(PET)_{15}(DG)_2]\cdot 4[DG]$ in chloroform. Inset shows a zoomed-in view of the region (2000-1750 cm^{-1}) which corresponds to intercluster ligand interactions brought about by dimerization. These peaks are notably absent in $[Au_{20}(PET)_{15}(DG)_2]\cdot 4[DG]$, further affirming its lack of dimerization/polymerization. See reference 2 for further details.

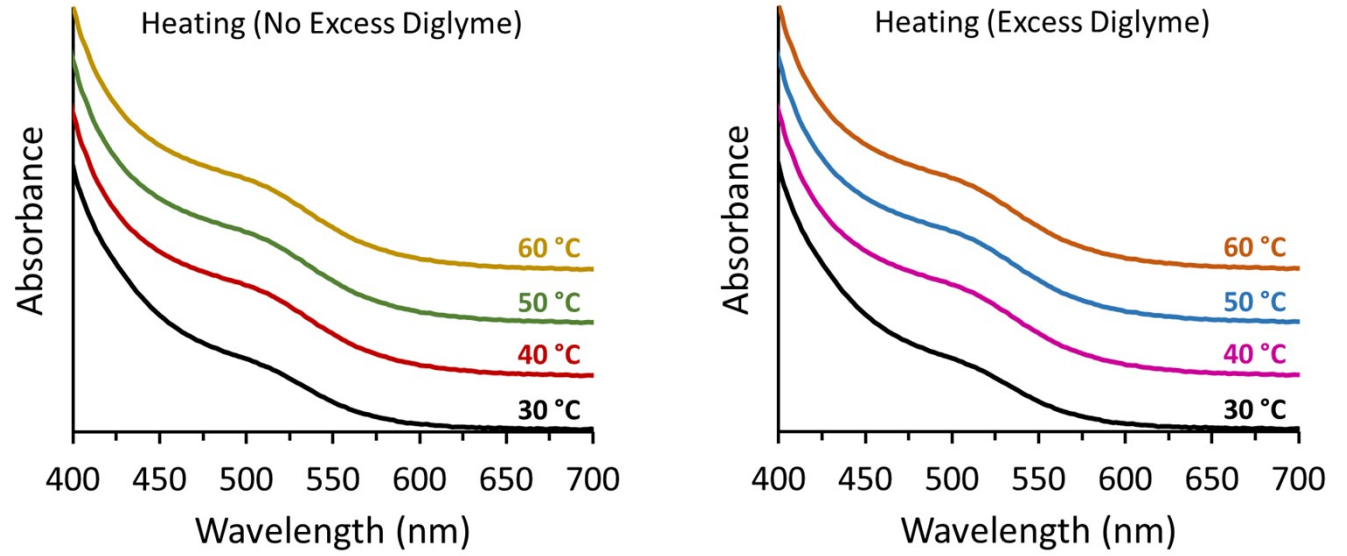

Figure S5: Stacked linear absorption spectra of $[Au_{20}(PET)_{15}(DG)_2]\cdot 4[DG]$ when exposed to different temperatures without (left) and with (right) excess diglyme.

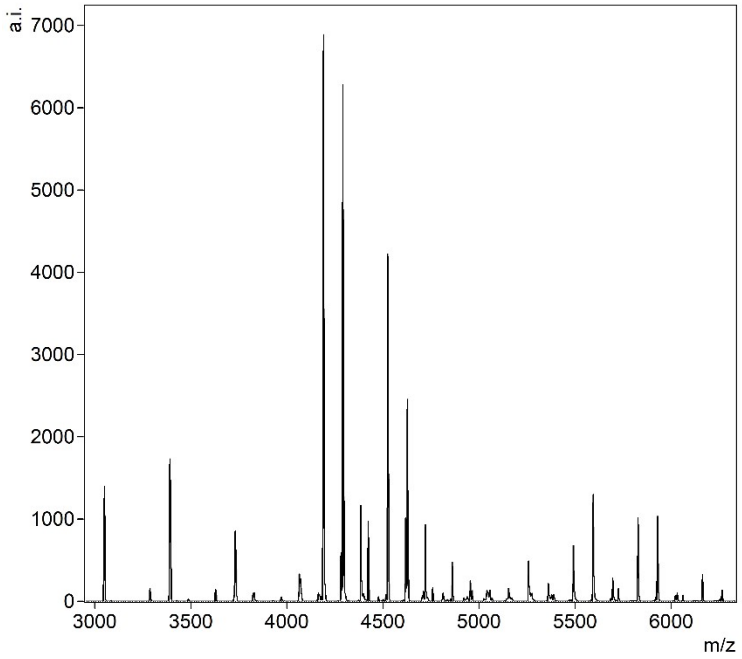

Figure S6: Full MALDI-MS spectrum of $Au_{20}(PET)_{15}(DG)_2]\cdot 4[DG]$ collected in the positive ionization mode.

References

1) Parker, J. F.; Weaver, J. E. F.; McCallum, F.; Fields-Zinna, C.A.; Murray, R. W. *Langmuir* **2010**, *26*, 13650.
2) Compel, W. S.; Wong, O. A.; Chen, X.; Yi, C.; Geiss, R.; Häkkinen, H.; Knappenberger, K. L.; Ackerson, C. J. *ACS Nano* **2015**, *9 (12)*, 11690–11698.

Computational Methods

NMR Calculations: Diglyme

Because the terminal methyl group of diglyme can rotate freely at room temperature, two structures for linear diglyme, labeled diglyme-GS and diglyme-TS (**Figure S7**), are considered. Diglyme-GS is the global minimum structure and diglyme-TS is a transition state related to rotation of the terminal methyl groups. Diglyme-GS is lower in energy than diglyme-TS by 18.9 kJ/mol.

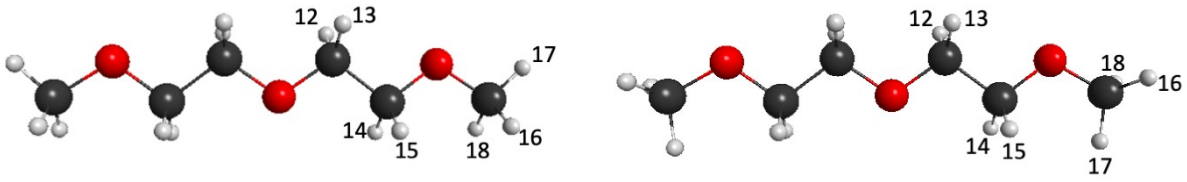

diglyme-GS **diglyme-TS**

Figure S7: Fully optimized BP86/TZP structures for diglyme-GS and diglyme-TS. These structures differ in the orientation of the terminal methyl groups. Hydrogen atoms are labeled 12, 13, 14, 15, 16, 17, and 18 respectively. Carbon = gray, oxygen = red, and hydrogen = white.

From **Table S1**, it can be noted that averaging the chemical shifts for diglyme-GS and diglyme-TS leads to chemical shifts that are consistent with the experimental results in Figure 2, as would be expected due to free rotation of the methyl groups. Thus, the calculated results are consistent with a linear diglyme molecule in pure solution indergoing free methyl rotation. Hydrogen atoms in CH_2 groups have chemical shifts at around 3.8 ~ 4.0 ppm, which are only about 0.4 ppm higher than those determined experimentally.

	hydrogen atom	chemical shifts (ppm)		hydrogen atom	chemical shifts (ppm)
	12	3.93		12	3.83
	13	3.93		13	3.83
	14	3.84		14	3.98
diglyme-GS	15	3.84	**diglyme-TS**	15	3.98
	16	3.56		16	3.97
	17	3.84		17	3.26
	18	3.56		18	3.97

Table S1: Calculated ^{1}H NMR chemical shifts for hydrogen atoms 12, 13, 14, 15, 16, 17, and 18 in diglyme-GS and diglyme-TS.

Binding Energy Analysis

To examine the binding strength between $Au_{20}(SCH_3)_{15}^+$ and diglyme, we consider the binding of these fragments to form the full $Au_{20}(SCH_3)_{15}DG^+$ system. The optimized $Au_{20}(SCH_3)_{15}DG^+$ coordinates (below) are split into fragments that are considered without further optimization (i.e. frozen fragments). We also fully optimize the fragments and determine the binding energy to form $Au_{20}(SCH_3)_{15}DG^+$. For diglyme, we consider the crown-like minimum similar to the arrangement on the nanoparticle (crown) and its global energy minimum (linear).

Optimization of diglyme changes the energy by less than 8 kJ/mol, whereas optimization of the $Au_{20}(SCH_3)_{15}^+$ fragment leads to an energy stabilization of 52.5 kJ/mol; indicating that the binding of diglyme has resulted in a significant geometrical rearrangement of the Au_{20} cluster compared to the structure without diglyme (**Table S2**).

		Frozen fragments	**Optimized fragments**	
Relative energies	$Au_{20}(SCH_3)_{15}^+$	52.5	0	
(kJ/mol)	DG	7.9	2.6 (Crown)	0 (Linear)
Binding energies (kJ/mol)		-204.7	-146.7	-141.8

Table S2: Relative energies of $Au_{20}(SCH_3)_{15}^+$ and diglyme fragments before and after fragment optimization, followed by binding energies of fragments to form $Au_{20}(SCH_3)_{15}DG^+$.

Optimized BP86/TZP coordinates for $Au_{20}(SCH_3)_{15}DG^+$:

Au 14.241138 11.425786 -0.092579

Au 14.660912 12.251971 3.376269

Au 16.246342 13.555258 0.224274

Au 15.895334 14.373573 -2.511098

Au 14.739907 15.898072 -0.469852

Au 15.684812 18.447517 2.438385

Au 13.357622 16.638112 1.762807

Au 14.164861 18.700721 -0.380090

Au 13.615731 21.571629 -0.053126

Au 12.310963 19.366933 2.574677

Au 14.470293 15.888862 4.558413

Au 15.939093 15.543087 2.062360

Au 13.904047 12.796653 -3.800841

Au 11.244799 14.259763 -0.652962

Au 13.762272 13.931420 1.325519

Au 12.692210 18.303376 -3.258133

Au	15.473678	16.989291	-2.913062
Au	15.343591	20.093681	-2.990275
Au	14.013887	16.035165	-5.496651
Au	13.240172	15.444077	-2.718252
S	14.836927	18.212715	4.606876
S	12.967591	21.574103	2.197114
S	16.460128	18.828150	0.257394
S	14.003806	13.657116	5.127302
S	15.421705	10.675476	1.811379
S	17.574291	12.867902	-1.671712
S	11.443013	17.236763	3.065730
H	12.061195	10.023818	-3.471969
S	13.423990	18.320889	-5.490587
S	14.184406	22.003524	-2.280891
S	11.940617	18.161298	-1.034916
S	14.506864	13.761899	-5.858877
S	12.877038	11.727478	-1.975290
S	11.384824	13.700205	1.607318
S	16.844719	18.587566	-4.019838
S	10.976345	14.635804	-2.950240
C	16.905591	20.608422	0.178889
C	12.165436	13.646304	5.097635
H	13.665115	9.550168	-2.820550
C	14.551742	21.750383	3.119739
C	16.288108	18.391074	5.728489
C	10.032291	17.017252	1.896996
C	17.065053	11.160699	-2.120637
C	14.473206	9.152202	2.261237
C	10.907944	19.635217	-0.683916

C	16.350309	13.741769	-5.919050
C	9.864873	16.093659	-3.088176
C	12.590019	21.883828	-3.194399
C	11.868748	18.334854	-6.484288
C	18.353644	18.662357	-2.961307
C	11.095849	11.883998	1.669764
C	12.693732	9.989524	-2.578533
H	17.848340	20.746363	0.720082
H	16.114603	21.236689	0.605082
H	17.030428	20.859166	-0.883251
H	11.822147	14.316358	5.893012
H	11.834541	12.622313	5.301230
H	11.797328	13.988813	4.124641
H	12.196949	9.410558	-1.792491
H	11.643352	11.387576	0.860694
H	10.020634	11.696309	1.578223
H	14.318957	21.661802	4.186365
H	14.961960	22.741840	2.900553
H	15.257908	20.959839	2.832803
H	15.949671	18.157163	6.743717
H	16.622164	19.433062	5.674753
H	17.080573	17.707985	5.411795
H	9.664892	15.995319	2.035944
H	10.366704	17.143878	0.862953
H	9.254587	17.744277	2.152649
H	15.975595	11.058294	-2.048762
H	17.554212	10.463863	-1.431420
H	17.395015	10.975475	-3.148867
H	14.858931	8.798646	3.223491

H	14.657315	8.403636	1.483764
H	13.404792	9.367760	2.338463
H	10.730543	19.650137	0.400927
H	9.963054	19.525015	-1.227671
H	11.420929	20.559184	-0.973534
H	16.769235	14.227523	-5.030354
H	16.650969	14.278155	-6.825171
H	16.670929	12.696095	-5.972078
H	10.082326	16.816798	-2.298277
H	8.833129	15.733954	-3.007158
H	10.031916	16.554702	-4.068272
H	12.164812	20.875920	-3.094189
H	12.811090	22.081876	-4.248762
H	11.909339	22.645408	-2.799685
H	11.190975	17.540997	-6.161467
H	12.149517	18.187700	-7.532724
H	11.398779	19.315596	-6.354579
H	18.085761	18.584182	-1.903406
H	18.867932	19.608311	-3.162983
H	18.992357	17.819468	-3.248070
H	11.468356	11.530702	2.638978
O	18.001130	16.277071	3.935011
C	18.661342	15.217199	4.645754
C	18.910697	17.160381	3.258313
C	19.411011	16.592543	1.943657
C	17.690795	14.061428	4.777501
O	18.290821	16.433157	1.078172
O	17.279126	13.544396	3.506028
C	18.666845	16.062500	-0.253199

C	18.293845	12.768751	2.851218
H	18.961022	15.568003	5.649615
H	19.572053	14.902429	4.112599
H	18.325427	18.070452	3.055280
H	19.761440	17.417687	3.910886
H	19.932439	15.626008	2.083290
H	20.137048	17.300525	1.502137
H	18.137703	13.262923	5.394090
H	19.110794	15.053924	-0.278686
H	19.383981	16.790841	-0.664840
H	17.749844	16.072652	-0.853987
H	18.610938	11.929666	3.490601
H	17.836576	12.382620	1.930680
H	19.167221	13.379677	2.576638
H	16.768288	14.411084	5.262760